Food Chemistry 433 (2024) 137275

Contents lists available at ScienceDirect

Food Chemistry

journal homepage: www.elsevier.com/locate/foodchem

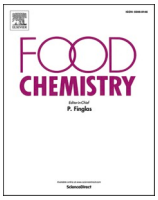

Sodium doping and trapped ion mobility spectrometry improve lipid detection for novel MALDI-MSI analysis of oats

Wai C.D. Lau [a], Leigh Donnellan [a], Matthew Briggs [a], Thusitha Rupasinghe [b], John C. Harris [c,d], Julie E. Hayes [d], Peter Hoffmann [a,*]

[a] UniSA Clinical and Health Sciences, Health and Biomedical Innovation, University of South Australia, Adelaide, South Australia 5000, Australia
[b] SCIEX, Australia
[c] South Australian Research and Development Institute, Department of Primary Industries and Regions, Adelaide, South Australia 5000, Australia
[d] School of Agriculture, Food and Wine, University of Adelaide, Waite Campus, Urrbrae, South Australia 5064, Australia

ARTICLE INFO

Keywords:
MALDI-MSI
TIMS
Oat
Lipids
Sodium doping
Isobaric and isomeric

ABSTRACT

Oat (*Avena sativa* L.) is an important cereal grain with a unique nutritional profile including a high proportion of lipids. Understanding lipid composition and distribution in oats is valuable for plant, food and nutritional research, and can be achieved using MALDI mass spectrometry imaging (MALDI-MSI). However, this approach presents several challenges for sample preparation (hardness of grains) and analysis (isobaric and isomeric properties of lipids). Here, oat sections were successfully mounted onto gelatin-coated indium tin oxide slides with minimal tearing. Poor detection of triacylglycerols was resolved by applying sodium chloride during mounting, increasing signal intensity. In combination with trapped ion mobility spectrometry (TIMS), lipid identification significantly improved, and we report the separation of several isobaric and isomeric lipids with visualisation of their "true" spatial distributions. This study describes a novel MALDI-TIMS-MSI analytical technique for oat lipids, which may be used to improve the discovery of biomarkers for grain quality.

1. Introduction

Matrix-assisted laser desorption/ionisation mass spectrometry imaging (MALDI-MSI) combines the analytical principles of MALDI mass spectrometry and microscopic visualisation to elucidate the spatial distribution of analytes *in situ*. MALDI-MSI has been commonly implemented in medical research for disease diagnosis, prognostic biomarkers identification and therapeutic discovery, but is also becoming more popular for agricultural and food science applications (Kokesch-Himmelreich et al., 2022; Yoshimura & Zaima, 2020).

Cereal grains are the most common food staple globally, providing an estimated 50% of human dietary energy (Laskowski et al., 2019). Compared to other cereal grains, oats (*Avena sativa* L.) have a distinct nutrient profile including significant amounts of dietary fibre (especially β-glucan), and unique protein and phytochemical (e.g. phenolic acids, vitamin E, avenanthramides and avenocosides) fractions (Gangopadhyay et al., 2015). Oats also have a high lipid content (~3 to 12% of the grain depending on variety) compared to other common cereals such as rice, wheat and barley, with a good proportion of unsaturated fatty acids (Zhou et al., 1999). This lipid fraction has important implications for the metabolizable energy value of oat as an animal feed, flavour and functionality of the grain and milled flour as a food ingredient, and its storage properties, with lipid oxidation or hydrolysis leading to the development of rancidity (Rasane et al., 2015).

Triacylglycerols (TGs) represent the main lipid class in oats, constituting up to almost 85% of total lipid. A further 6 to 26% of oat lipids are phospholipids, mostly in the form of phosphatidylcholine (PC) and phosphatidylethanolamine (PE) (Zhou et al., 1999). MALDI-MSI has been used to investigate lipids in cereals including wheat, barley and rice, mainly in relation to plant growth and development (Feenstra et al., 2017; Gorzolka et al., 2016), and these studies were mainly focussing on phospholipid detection. However, MALDI-MSI has not been applied to oat samples, despite the high lipid content of oat grains having significant implications for food processes.

Lipid MALDI-MSI of oats presents multiple challenges before and during analysis. The first step of sample preparation typically involves: (i) tissue sectioning, (ii) section mounting and (iii) matrix deposition (Dong et al., 2016). The hardness and low tissue moisture of grains can

* Corresponding author.
E-mail address: peter.hoffmann@unisa.edu.au (P. Hoffmann).

https://doi.org/10.1016/j.foodchem.2023.137275
Received 23 May 2023; Received in revised form 8 August 2023; Accepted 22 August 2023
Available online 26 August 2023

cause tissue rupture during sectioning and poor adherence onto indium tin oxide (ITO) glass slides used for MALDI-MSI, resulting in cracks and shrinkage of the tissue upon matrix deposition (Boughton et al., 2015). Another major challenge that arises during lipid MALDI-MSI is the extreme structural diversity of this analyte, thus rendering a high number of isobaric and isomeric lipid species with overlapping masses, thereby limiting the accuracy in molecular identification (Helmer et al., 2021). Changes in lipid signal intensities and distribution have been observed in previous MALDI-MSI analysis of grains at different storage years (Zhang et al., 2023), germination stages (Gorzolka et al., 2016) and the presence of fungal infection (Righetti et al., 2022), suggesting the potential of lipids as biomarkers for grain quality. However, the possibilities of mis-annotating isobaric/isomeric lipids were not addressed. Moreover, the detection of neutral lipids, such as TGs, is known to be limited due to the instability of protonated TG adducts (Gorzolka et al., 2016; Leopold et al., 2018). Therefore, more innovative techniques are required to enable lipid MALDI-MSI analysis of oat grains that can provide greater confidence in lipid identification.

The recently developed timsTOF *flex* instrument offers a state-of-the-art MALDI-time-of-flight (TOF)-MSI platform with the option to activate trapped ion mobility separation (TIMS), a relatively new gas-phase ion-mobility separation feature. The activation of TIMS can be beneficial as it allows greater differentiation of lipids with very similar mass-to-charge (m/z) ratios, whereby isomeric and isobaric lipids can be further separated prior to detection. In brief, TIMS enables the acquisition of a collision cross-section (CCS) value measured in units of square angstroms ($Å^2$), as determined by the three-dimensional structural conformation of an ionised analyte. In combination with accurate mass measurements, CCS values can be used to improve the accuracy and specificity of ion identification in complex samples (Paglia et al., 2015; Paglia et al., 2014). This is particularly beneficial for the differentiation of isobaric and isomeric lipids, which can now be resolved in the gas phase (Spraggins et al., 2019).

In this study, we aim to establish a MALDI-MSI method for the analysis of lipids in oats, focussing on TG and phospholipid classes. This includes optimising sample preparation techniques for oat grains to preserve tissue morphology and adherence on ITO slides, as well as improve detection of TGs. Using the optimised methods, distinct localisation patterns of isobaric and isomeric lipids in oats were also explored with the application of TIMS for the first time ever.

2. Materials & methods

2.1. Reagents & materials

MALDI matrix 9-aminoacridine (9AA, #92817), gelatin powder (#G2500), chromium potassium sulfate dodecahydrate (#243361), sodium carbonate (Na_2CO_3, #S7795), sodium acetate (NaAce, #S8750), red phosphorus (#343242) and trifluoroacetic acid (TFA, #302031) were purchased from Sigma-Aldrich (St. Louis, USA). Sodium chloride (NaCl, #SA046) was purchased from ChemSupply. MALDI matrices α-Cyano-4-hydroxycinnanic acid (HCCA, #8201344) and 2,5-dihydroxybenzoic acid (DHB, #8201346) were purchased from Bruker Daltonics (Germany). Methanol (MeOH) and acetonitrile (ACN) were purchased from Supelco (Pennsylvania, USA). ESI-L Low Concentration Tuning Mix (#G1969) was purchased from Agilent Technologies (California, USA). A sample of de-hulled, commercial milling-grade Australian oat (*Avena sativa*) was used for this study, with a total lipid content of 7.7% (ALS Food & Pharmaceutical, Victoria).

2.2. Lipid extraction from oats

Lipids were extracted from oat grains according to a previously established Blight and Dyer method with minor modifications. Oat grains (2 g) were crushed to a fine powder using a mortar and pestle. Chloroform:methanol solution (1:1 ratio, 20 mL) was added to the oat flour and vortexed for 2 min. Saturated NaCl (4 mL) was then added into the mixture and left aside for phase separation. After 30 mins, a Pasteur pipette was used to carefully remove the upper methanol layer. The bottom chloroform layer was collected and filter-sterilised to remove all solid particles. Lipid extract was concentrated in a SpeedVac for 1 h at 50 °C and stored at −80 °C until further use. Lipid extract was reconstituted in chloroform to 50 mg/mL for MALDI-MS analysis.

2.3. HPLC-MS/MS data acquisition and analysis

Lipid extract was reconstituted in butanol:methanol (1:1) in ammonium acetate (10 mM) before high performance liquid chromatography (HPLC) separation on a Shimadzu Nexera LC 40D X3 system using a Phenomenex Kinetex C18 column. A total volume of 5 μL was injected. Ammonium acetate (10 mM) in isopropanol, acetonitrile and water (2:3:5 v/v/v) was used as mobile phase A, while ammonium acetate (10 mM) in isopropanol, acetonitrile and water (9:0.9:0.1 v/v/v) was used as mobile phase B, with a flow rate of 0.400 mL/min. MS data were simultaneously acquired with a TOF MS scan range of 100–1600 Da, and a TOF MS/MS scan range of 100–1500 Da, using a SCIEX ZenoTOF 7600 system (SCIEX, Massachusetts, USA). MS data acqusition was carried out using Zeno Trap active with fragmentation using Electron Activated Dissociation (EAD) with Independent Data Acqusition (IDA). Mass spectrometry parameters were a declustering potential of 80 V, ion source gas 1 (GS1) at 55 psi and ion source gas 2 (GS2) at 65 psi with source temperature of 250 °C. For EAD fragmentation, Electron Kinetic Energy was used at 15 eV with electron beam current at 7000nA. Data were processed using MS-DIAL software (version 5.1.0, RIKEN, Japan) for lipid annotations.

2.4. Preparation of gelatin-coated ITO slides

Gelatin-coated ITO slides were prepared according to our previously published method (Lee et al., 2021). Gelatin solution (0.5% w/v) was prepared in Milli-Q water at 40 °C and chromium potassium sulfate dodecahydrate (0.05% w/v) was added. The gelatin solution was filter-sterilised and conductive ITO slides were dipped into the solution for 10 s before drying overnight at room temperature.

2.5. Tissue sectioning and mounting

Oat grains were freshly embedded in 10% gelatin and left at −20 °C in a Leica cryostat for temperature equilibration. After approximately 1 h, grains were sectioned at various thicknesses, with 25 μm identified as the optimum thickness. Oat sections were mounted onto gelatin-coated ITO slides and a 0.5 μL droplet of milliQ water or salt solution (100 mM NaCl, 100 mM NaAce or 50 mM Na_2CO_3) was added directly onto the section. After mounting, oat sections were immediately transferred to a dessicator for overnight drying.

2.6. Matrix deposition

Matrix solutions used in this study were prepared as follows: 10 mg/mL 9AA in 70% MeOH (w/v), 30 mg/mL DHB in 50% MeOH (w/v) and 10 mg/mL HCCA in 50% ACN (w/v). TFA at a final concentration of 0.2% was added into all matrix solutions. For MALDI-MS experiments, lipid extracts from oats (n = 3) were reconstituted in chloroform to 20 mg/mL and mixed with matrix solutions (9AA, DHB or HCCA) at a 1:1 ratio, before being spotted onto a MALDI Target Plate (MTP) 384 polished steel (Bruker Daltonics, Germany). For MALDI-MSI analysis, HCCA matrix solution was sprayed onto oat sections using an iMatrixSpray instrument, as described in our previously established protocol (Lee et al., 2021).

2.7. MALDI-MS data acquisition and analysis

All MS data were acquired using the timsTOF *flex* mass spectrometer (Bruker Daltonics) controlled by timsControl (version 3.0.21, Bruker Daltonics) and FlexImaging (version 7.0, Bruker Daltonics) in positive ionisation mode, within the mass range of *m/z* 300 to 1300 with a spatial resolution of 20 μm. Instrument-specific settings were as follows: 350 Vpp tunnel RF, 10 eV collision energy, 2500 Vpp collision RF, 5 eV ion energy, 80 μs transfer time, 10 μs pre pulse storage. A total of 200 shots were acquired at each pixel. Prior to data acquisition, the timsTOF fleX instrument was calibrated using red phosphorus for MALDI-MSI and Tuning Mix for MALDI-TIMS-MSI.

MALDI-MS data were analysed using DataAnalysis (version 6.0, Bruker Daltonics). MALDI-MSI data were processed using SCiLS Lab (version 2023a Pro, SCiLS, Bruker Daltonics) and MetaboScape (version 6.0.2, Bruker Daltonics) for preliminary lipid annotations. Hotspot removal was applied and normalised to the 99% quartile during ion image generation. Two methods were implemented to annotate lipids: (i) Rule-based annotation and (ii) Spectral List annotation (LIPID MAPS® Structure Database (LMSD)). For tolerances and scoring parameters, a mass error within the range of 10 ppm was set for MALDI-MSI and MALDI-TIMS-MSI analyses. Three biological replicates were analysed for all experiments and lipids that were annotated in only one replicate were rejected. Ion intensity maps were then generated in SCILS Lab based on annotations imported from MetaboScape to visualise spatial distribution of specific lipids. Data was normalised to total ion count and ion intensity maps were weakly denoised with automatic hotspot removal.

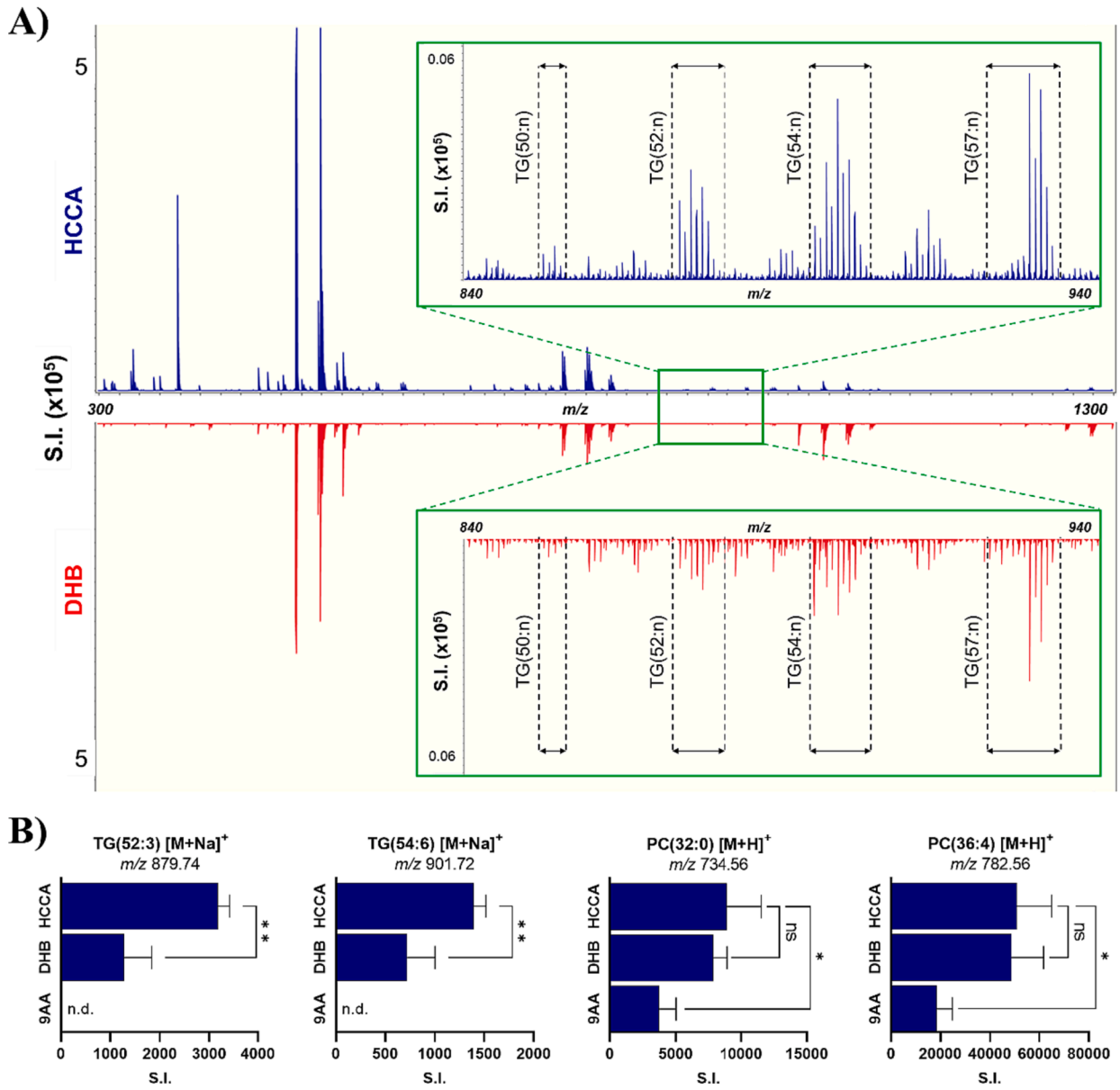

Fig. 1. Optimisation of matrix solutions on lipid extracts from oats for MALDI-MSI analysis. (A) Mass spectra acquired from lipid extracts from oats via MALDI-MS with the application of HCCA and DHB. Mass range of *m/z* 840 – 940 is magnified (green box) to highlight the general range of TGs. n, number of carbon–carbon double bonds. (B) Signal intensities of selected triacylglycerols [TG(52:3) $[M + Na]^+$ & TG(54:6) $[M + Na]^+$] and phosphatidylcholines [PC(32:0) $[M + H]^+$ & PC (36:4) $[M + H]^+$] acquired from lipid extracts overlaid with HCCA, DHB and 9AA matrices. Experiments were performed in triplicates. S.I., signal intensity. *, ** indicate significant correlations at $p < 0.05$ and $p < 0.01$, respectively. (For interpretation of the references to colour in this figure legend, the reader is referred to the web version of this article.)

3. Results & discussion

3.1. Optimising matrices for lipid MALDI-MS anaysis of oat extracts

The matrix serves as a critical compound to promote the desorption and ionisation of the analytes of interest in MALDI experiments (Sturtevant et al., 2015). The choice of matrix must be optimised for different analytes as an incompatible matrix can cause a decrease in resolution and ionisation efficiency of analytes (Leopold et al., 2018). Prior to lipid MALDI-MSI, different matrices (DHB, HCCA, and 9AA) were tested on lipid extracts from oats to determine the most suitable matrix with maximum ionisation efficiency and signal-to-noise ratio. The concentrations used for each matrix were determined based on a previous MALDI-MSI study, which provided the highest signal intensities for cereal lipids (Zhang et al., 2023). In this study, mass spectra for lipid extracts overlaid with HCCA were compared to extracts overlaid with DHB and 9AA. In comparison to DHB, HCCA produced higher signal intensities for oat lipid extracts, especially within the mass range of *m/z* 840 to 950 where several TG species can be found (Fig. 1A). 9AA, however, resulted in poor ionisation and signal intensity (Fig. S1).

Two TGs (TG(52:3) $[M + Na]^+$, MS1: *m/z* 879.74; TG(54:6) $[M + Na]^+$, MS1: *m/z* 901.72), and two PCs (PC(32:0) $[M + H]^+$, MS1: *m/z* 734.56; PC(36:4) $[M + H]^+$, MS1: *m/z* 782.56), all with different saturation degrees, were selected to assess signal quality between different matrix solutions (Fig. 1B). It was evident that significantly higher signal intensities of TGs were acquired from lipid extracts overlaid with HCCA. While signal intensities of selected PCs appeared to be higher in HCCA-coated samples than those overlaid with DHB, the differences were not significant. With a focus on TG and PC lipids, HCCA was used as the matrix of choice for lipid MALDI-MSI of oats in further experiments.

3.2. Optimising sample preparation for MALDI-MSI of oats

Optical images of the ventral and dorsal sides of an oat grain are shown in Fig. 2A. Preparation of oat sections must be managed with high precautions as it affects the quality and resolution of the downstream MSI analysis. The hardness of the seed coat and brittleness of the grain have rendered it difficult to obtain thin sections without compromising the morphology. Therefore, the choice of embedding material and section thickness are important factors to consider during oat sectioning. Gelatin (10%) (Fenyk et al., 2022; Liu et al., 2021; Woodfield et al., 2017) and CMC (2%) (Montini et al., 2020; Yoshimura et al., 2012) were assessed for suitability as embedding materials for grains in MALDI-MSI experiments. In this study, 10% gelatin was preferred, as we failed to obtain any whole tissue section with 2% CMC (data not shown). The embedded grains were sectioned at different thicknesses, and intact sections were consistently obtained when 25 μm thickness was used (Fig. S2A).

Another caveat for oats sections was the lack of adherance to ITO slides, which resulted in the tearing and shrinkage of sections during matrix deposition. We previously demonstrated that the coating of ITO slides with 0.5% gelatin improved the morphology and adhesion of cartilage-bone tissue (Lee et al., 2021), which is also brittle and prone to cracking, and hence we reviewed the suitability of gelatin-coated ITO slides for maintaining oat tissue morphology. As shown in Fig. S2B, gelatin-coated ITO slides increased the adherence of oat sections, however, fractures were still visible. Following further optimisation, it was determined that the subsequent addition of a small water droplet after mounting on gelatin-coated ITO slides significantly improved tissue morphology and adherence.

This was followed by the deposition of the optimised HCCA matrix onto the section, which would co-crystallise with lipids on the tissue surface. This aids in the desorption and ionisation of lipid molecules to be analysed by mass spectrometry. In this study, we trialled two different instruments for matrix deposition and compared the effects on the oat sections. The iMatrixSpray instrument was preferred for matrix coating as it alleviated tissue shrinkage issues that were observed when matrix was deposited via ImagePrep (Fig. S2B).

Fig. 2B illustrates the three main parts of the grain: endosperm, bran and embryo. The starchy endosperm makes up most of the grain, which is separated from the outermost bran by the aleurone layer. An intermediary layer isolates the endosperm from the embryo, which mainly consists of the scutellum and the embryonic axis. By applying the optimised sample preparation methods, mass spectra with similar peak patterns were acquired from the endosperm (Fig. S3A) and embryo (Fig. S3B) regions of oat sections mounted onto gelatin-coated and conventional ITO slides, demonstrating that gelatin-coating did not cause any interference with ion signals.

3.3. Sodium doping promotes TG ionisation in MALDI-MSI of oats

Using the optimised methods, we performed MALDI-MSI analysis of oat sections on our timsTOF *flex* instrument. The mass range of *m/z* 300 – 1000 is displayed in Fig. 3A, with the two main peak clusters under the

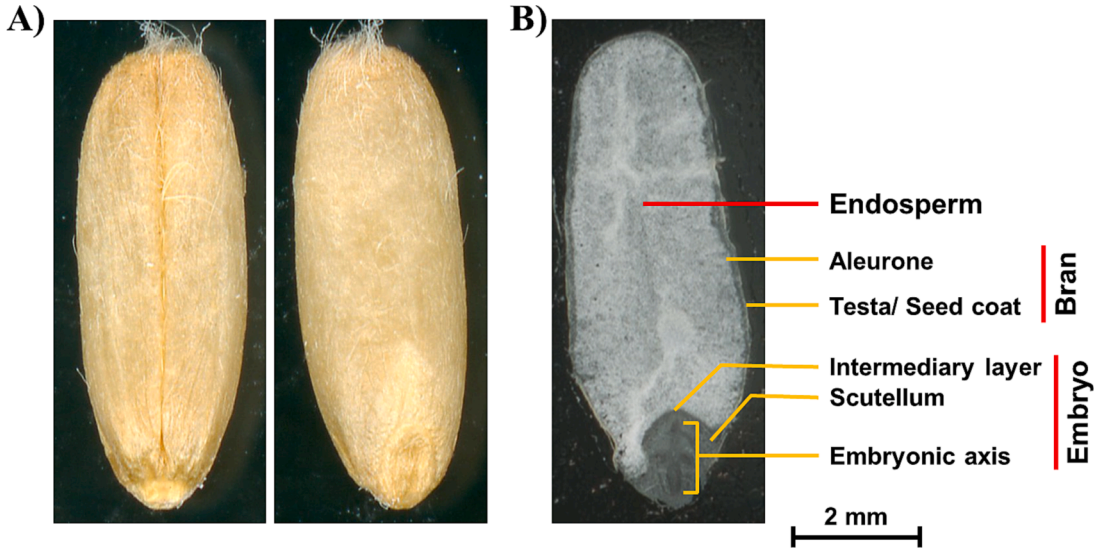

Fig. 2. Morphological features of oat grain. (A) Ventral (left) and dorsal (right) view of oat grain. (B) General histology of oat grain sectioned at 25 μm thickness. The endosperm, embryo (intermediary layer, scutellum & embryonic axis) and bran (aleurone & seed coat) make up the three main structures of an oat grain.

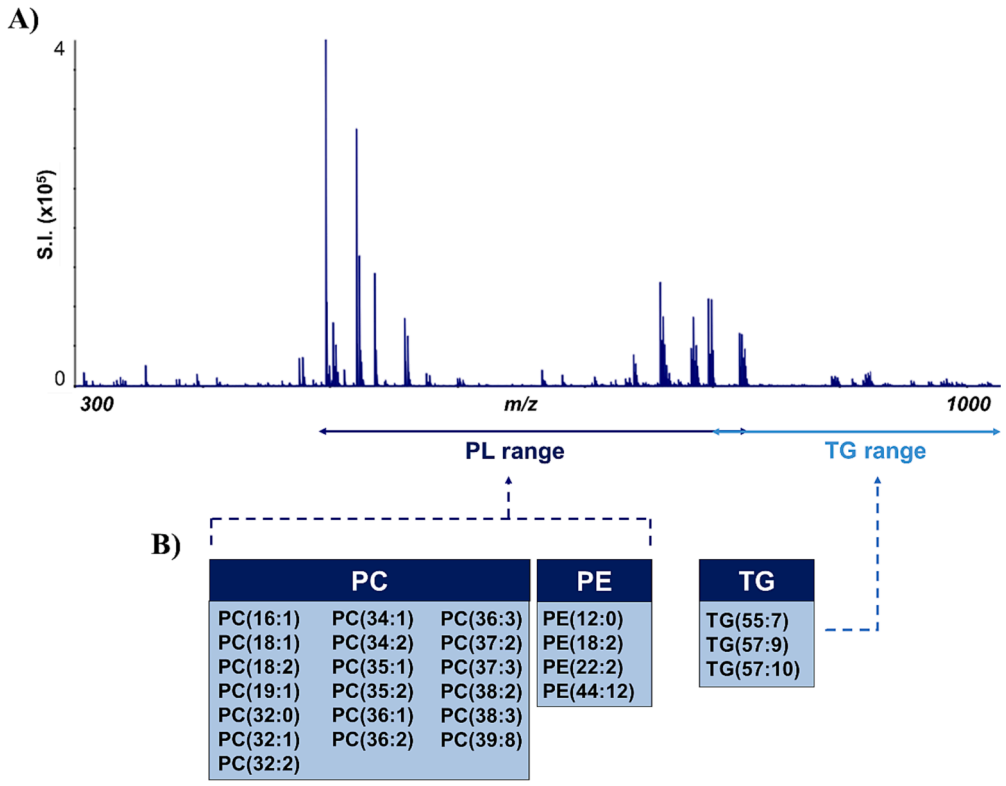

Fig. 3. MALDI-MSI of lipids in oats. (A) Mass spectra acquired from MALDI-MSI of whole oat sections using an optimised protocol. (B) List of PC, PE and TG lipids tentatively annotated using the MetaboScape platform.

'PL range' mainly correlated with PC and PE signals. Similar to previous studies, PLs are the dominant lipid species detected by MALDI-MSI, with a total of 19 PCs and 4 PEs annotated from two or more biological replicates (Fig. 3B). Despite being known as the major lipid component of oats, only 3 TGs were tentatively identified, all in the form of sodium adducts. The limited number of TGs identified may be due to signal suppression by easily ionised PC species and/or instability of protonated TG species (Leopold et al., 2018). Furthermore, the detection of lipids with odd-numbered fatty chains in plant matrices may be rare, but recent literature have suggested evidence for their presence in plant oils (Dąbrowski & Konopka, 2022). This highlights potential misassignment of lipid identifications and the importance of additional experiments to confirm their identities. While we reported all putative lipid identifications generated using MetaboScape, the lipids selected for distribution were first confirmed via HPLC-MS/MS.

It is known that TGs are observed exclusively in the form of alkali metal ($Li^+/Na^+/K^+$) or ammonium (NH_4^+) adducts, as protonated TGs fragment rapidly before they can be detected (Leopold et al., 2018). Matrix additives are often used during MALDI analysis to increase ionisation efficiency of certain analytes. Using salt as a MALDI matrix additive can improve detection of glycans (Kim et al., 2016), amino acids (Amiri et al., 2021) and lipids (Gidden et al., 2007). A previous study by Dufresne and colleagues demonstrated that the application of sodium allowed MALDI-MSI detection of neutral lipids including TGs (Dufresne et al., 2019). To improve the detection of TGs in our experiments, we replaced the 0.5 μL water droplet added during the section mounting step with NaCl (100 mM), NaAce (100 mM) or Na_2CO_3 (50 mM) solutions as Na^+ dopants. Within the mass range of *m/z* 840 to 950, multiple peaks that correlate to sodiated adducts of TG(50:n), TG(52:n), TG(54:n) and TG(57:n) could be observed after the addition of NaCl (Fig. 4A), Na_2CO_3 and NaAce (Fig. S4).

In general, sodium doping enabled the generation of more lipid annotations in oat sections, particularly TGs and other phospholipids such as phosphatidic acid (PA), phosphatidylglycerol (PG) and phosphatidylinositol (PI) (Fig. S5). The annotations were compared and presented in Venn diagram format, which indicated a better overall detection coverage for TG and PE (Fig. 4B), as well as other minor phospholipids (PA, PI, PG; Fig. S6) using NaCl. Different concentrations of NaCl were then screened for optimal TG detection. With increasing NaCl concentration the number of identified TG and PE species decreased, with an opposite trend observed for the others (Fig. S5).

Ion images were generated for three sodiated TG adducts in both water- and NaCl-doped samples (Fig. 4C), demonstrating the restricted detection of TGs when water is used and resolution with the use of NaCl (100 mM). The TGs were consistently localised around the endosperm, supporting previous studies in which oat oil was mainly found in the outer endosperm region of oat grains (Banaś et al., 2007; Heneen et al., 2009). The identities of the selected TG adducts were confirmed via HPLC-MS/MS analysis of oat lipid extracts as sodium or ammonium adducts (Fig. S7). On top of the comparison of MS/MS spectra, as presented in Fig. S7, lipid identities were also confirmed through the matching of measured retention time and mass accuracy with publicly available libraries integrated in MS-DIAL (Tsugawa et al., 2015). Given that TGs are the principal lipid class in oats, 100 mM of NaCl was selected as the optimum condition for section mounting.

3.4. Trapped ion mobility spectrometry (TIMS) activation improved lipid detection

In TIMS, ions are first trapped and accumulated in a high-pressure region before being released into a low-pressure region, where they are separated based on their mobility. The separation is achieved using a combination of a gas flow and an electric field, which causes the ions to move through a drift region at different rates depending on their size, shape and charge (Ridgeway et al., 2018). The ions are then detected and their *m/z* ratios are measured using a mass spectrometer. By introducing this additional separation step, TIMS can increase the peak capacity of mass spectrometry-based methods, allowing for the

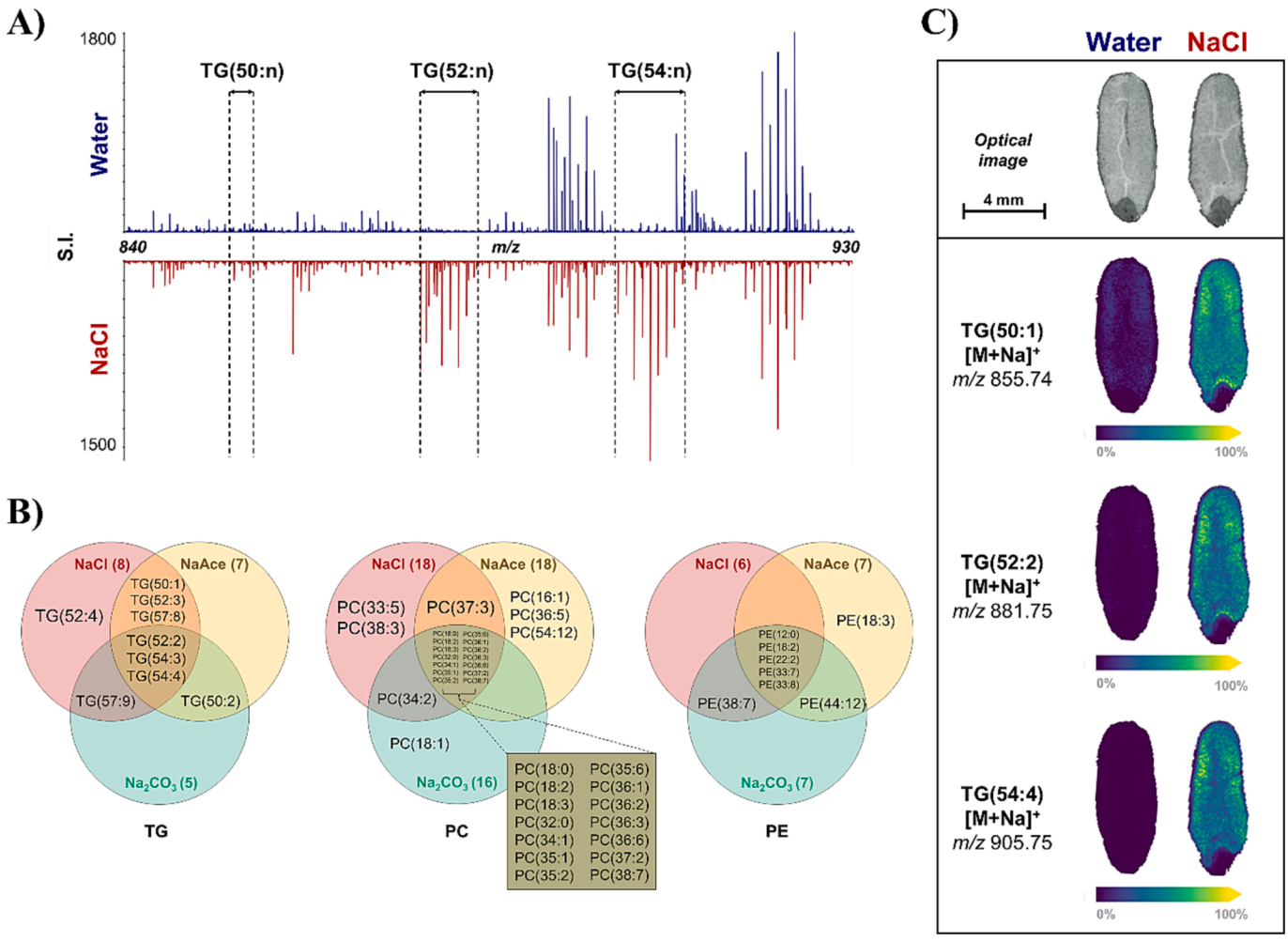

Fig. 4. Sodium doping promotes MALDI-MSI of TGs in oats. (A) MALDI-MSI spectra of *m/z* 840 to 930 acquired from oat sections, comparing the addition of water and 100 mM NaCl during section mounting. (B) Venn diagrams comparing lipids (TG, PC and PE) putatively annotated from NaCl-, NaAce- and Na_2CO_3-doped samples. (C) Ion distribution images of different TG species when water or NaCl (100 mM) was added.

detection and identification of more compounds in complex samples. Additionally, TIMS can increase the sensitivity of detection by reducing background interference and improving signal-to-noise ratios, which can be especially useful for low-abundance or trace-level analytes (Fu et al., 2020).

We examined whether TIMS activation would be beneficial for lipid analysis of oat sections. As expected, the activation of TIMS generated more than 10-fold higher signal intensities compared to when TIMS was not applied (Fig. S8). In the TIMS dimension, ions are temporally confined and accumulated within the ion funnel before being released subsequently into the TIMS analyser (Michelmann et al., 2015; Ridgeway et al., 2018). This reduces the loss of ions prior to detection by the analyser, which may explain the improved sensitivity. Around 300 lipids were tentatively identified in TIMS-activated replicates, including 29 TGs, 28 PCs, 4 PEs, 14 PAs, 11 PGs, 10 PIs and 10 phosphatidylserines (PSs) (Fig. 5A). The application of TIMS in the presence of NaCl also seemed to provide a comprehensive coverage for TGs, where 18 TGs were identified in addition to all 11 TGs detected in previous sections (Fig. 5B). Of all lipids, TIMS activation appeared to be the most beneficial for TG detection, suggesting the increased sentivity of MALDI-TIMS-MSI in picking up low-abundant TG signals that were originally suppressed by ionisation of phospholipids (Boskamp & Soltwisch, 2020). A list of all tentatively identified lipids from MALDI-TIMS-MSI of NaCl-doped samples can be found in Table S1.

Ion images corresponding to selected TGs and PCs (Fig. 5C), as well as other tentatively identified minor phospholipids (Fig. S9), were reconstructed, which corroborated the endosperm as the primary region for lipid storage in oat grains. However, it is worth noting that the spatial distribution of lipids is not restricted to the oat endosperm, as ion signals were also detected at a lower intensity in the embryo for several lipid species. The distinct localisation of PG(44:2) $[M + H]^+$ was also an intriguing finding, as it was distrubuted primarily in the embryo (Fig. S9). HPLC-MS/MS was performed to confirm the identities of the major lipids selected for ion image generation (Fig. S10). These results suggest the effectiveness of our MALDI-MSI sample preparation protocol, in combination with sodium doping and TIMS activation, for enhanced lipid identification and distribution analysis of oats.

3.5. *TIMS activation revealed distinct localisation of isobaric and/or isomeric oat lipids*

The isobaric and isomeric properties of lipids could result in their misannotations or misinterpretations of their "true" spatial distributions. In addition to increased sensitivity described in the previous section, TIMS could also resolve this issue by providing an additional dimension for the differentiation of isobaric and isomeric lipids based on their ionic conformations. Isobaric and isomeric molecules may share the same *m/z* value, but a difference in physiochemical properties can give rise to multiple conformations that can be measured as collision cross section (CCS) values (Paglia et al., 2015; Paglia et al., 2014). This

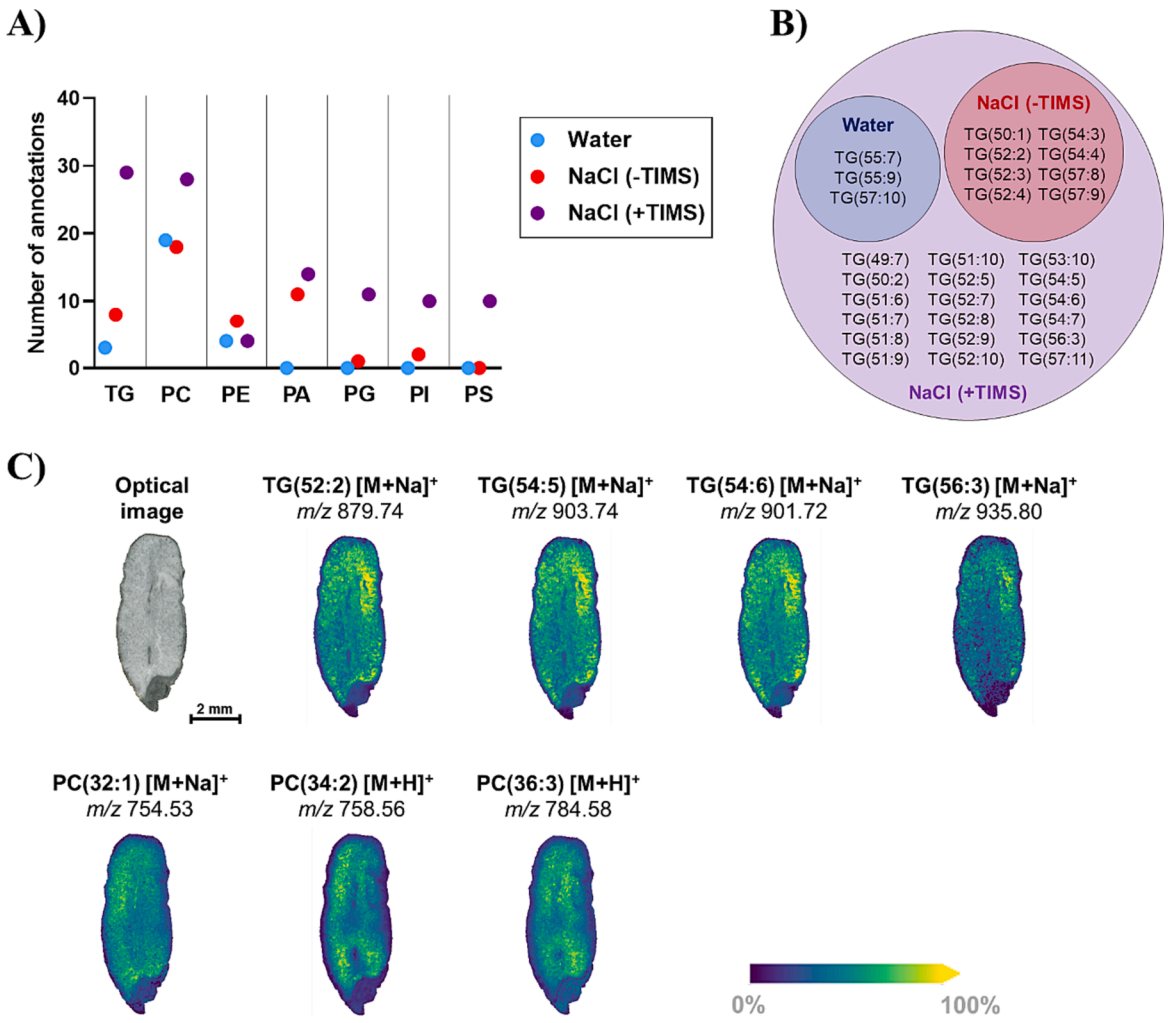

Fig. 5. MALDI-TIMS-MSI of lipids in oat sections. (A) Dot plot comparing the number of lipid annotations generated in water-doped oat tissue, as well as NaCl-doped samples in the presence and absence of TIMS activation. (B) Venn diagram comparing TG species identified in water-doped oat tissue, as well as NaCl-doped samples in the presence and absence of TIMS activation. (C) Ion images generated for selected TG and PC lipid species.

provides an additional parameter next to *m/z* value to improve the confidence of metabolite annotations.

Two distinct conformations corresponding to *m/z* 756.55 could be observed (Fig. 6A) via MALDI-TIMS-MSI of an oat section displayed in Fig. 6B. The major conformation (CCS: 291.71 $Å^2$) appeared to be distributed across the whole section, with higher signals acquired around the embryo region, while the minor conformation (CCS: 284.71 $Å^2$) predominantly localised in the endosperm only, in an even manner (Fig. 6C). HPLC-MS/MS data interrogation revealed that PC(34:3) $[M + H]^+$, as well as PC(32:0) $[M + Na]^+$, both have *m/z* value of 756.55 (Fig. 6D). By cross-referencing with previously determined CCS values (May et al., 2014), we are able to match the major conformation to PC (32:0) $[M + Na]^+$ and the minor conformation to PC(34:3) $[M + H]^+$, with a CCS tolerance of <2%.

A very similar case was also observed for isobaric lipids of *m/z* 782.56 (Fig. S11), in which the major conformation (CCS: 294.27 $Å^2$) was matched to PC(36:4) $[M + H]^+$, while the minor conformation (CCS: 288.22 $Å^2$) was matched to PC(34:1) $[M + Na]^+$ (May et al., 2014; Vasilopoulou et al., 2020). Other examples of unannotated isobaric or isomeric lipids that exhibit distinct localisation patterns are shown in Fig. S12.

A significant advantage of MALDI-MSI compared to traditional LC-MS/MS is the capability to visualise spatial information of metabolites, thus enabling a deeper level of understanding of their functional roles. Several MALDI-MSI studies have highlighted lipids as potential biomarkers for agricultural and food science applications. For instance, mycotoxin treatment induced region-specific accumulation of PCs in wheat plants (Righetti et al., 2021), suggesting physiological roles of certain lipids in response to fungal infection. In addition to PCs, phospholipids from PA and PI classes have been reported in the mycotoxin-infected plants, but not in the untreated control (Righetti et al., 2021), further corroborating that lipids may be used to predict microbial contamination. Another example was for the investigation of sensory or nutritional quality. Oxidation of lipids occur over time, which is a major factor of rancidity and undesirable taste. It was demonstrated that the signal intensities of lipids with unsaturated fatty acid chains decrease in rice grains as storage time increases. However, this phenomenon has not been observed in lipids with only saturated fatty acid chains (Zhang et al., 2023), implying that oxidation of lipids may have occurred. Nonetheless, most of these studies have not addressed the potential misinterpretation of isobaric or isomeric lipids and their distributions. In our study, a greater number of lipids were identified by combining sodium doping and TIMS during MALDI-MSI analysis of oats, which improves the likelihood of discovering new biomarkers tailored to specific applications. The value of MALDI-TIMS-MSI in resolving isobaric or isomeric molecules in oats was also demonstrated to provide more accurate information on lipid identification and spatial distribution.

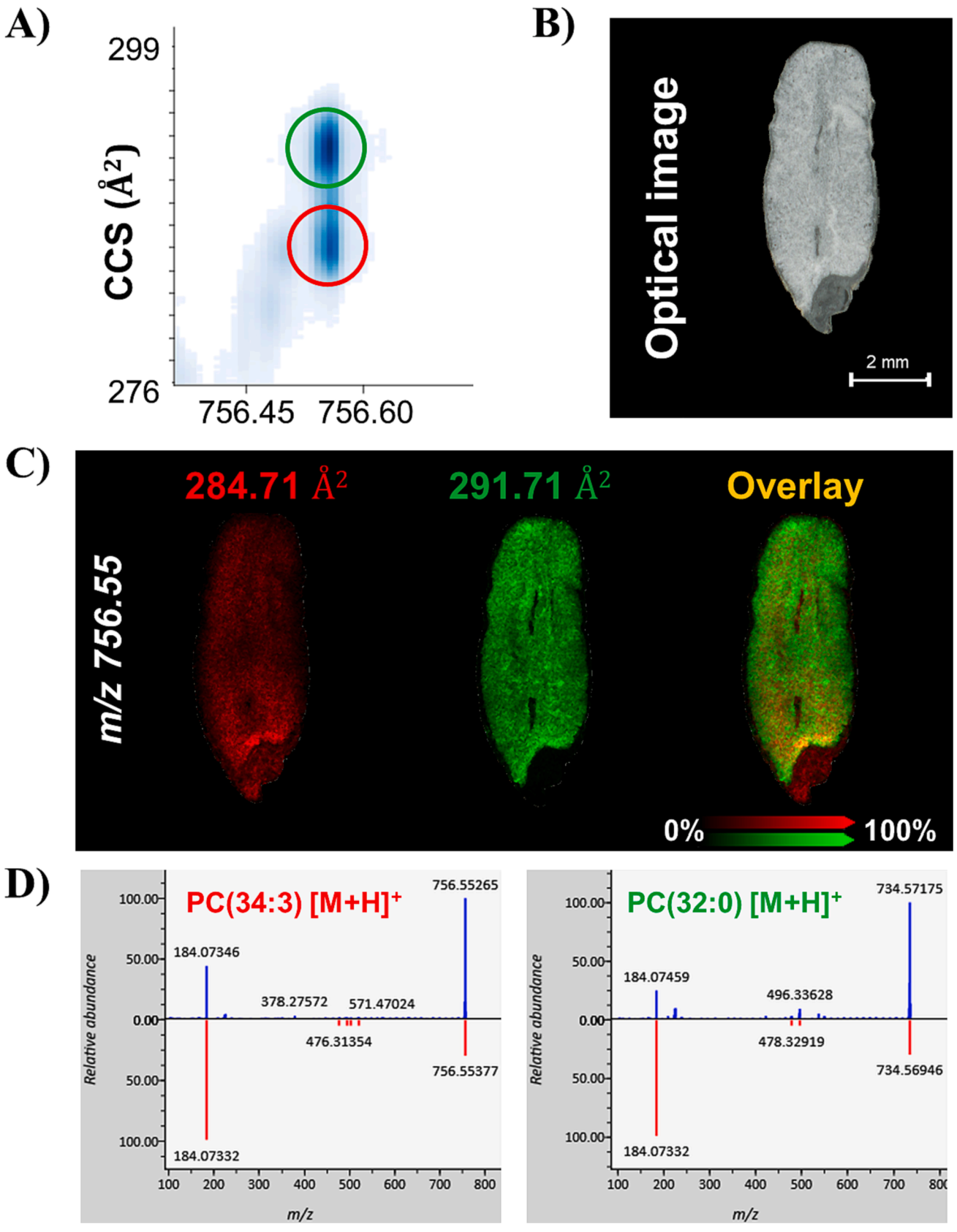

Fig. 6. TIMS activation revealed distinct localisation of isobaric oat lipids. (A) Ion mobility separation of two ion conformations with *m/z* 756.55. (B) Optical image of an oat section analysed via MALDI-TIMS-MSI. (C) Ion images of each conformation with an overlaid display. (D) HPLC-MS/MS determination of lipids present in oats with *m/z* value of 756.55. Protonated adduct of PC(34:3) and sodiated adduct of PC(32:0) would both have *m/z* 756.55. Measured spectrum (blue) was compared to reference spectrum (red) for confirmation of lipid identity. (For interpretation of the references to colour in this figure legend, the reader is referred to the web version of this article.)

4. Conclusion

There is limited knowledge of the spatial distribution of lipids in oat grains. From previous MALDI-MSI studies of cereal lipids, we acknowledged the potential importance of understanding lipid distribution for cereal crop physiology and food and ingredient research. Oats are of high scientific interest due to their high content and unique profile (high proportion of TGs) of lipids. Here we describe a novel lipid MALDI-MSI analysis pipeline for oat grains with a focus on the identification and detection of TGs and PCs, the main lipid classes of interest in the context of food. During sample preparation, HCCA was selected over DHB and 9AA as the matrix of choice for the detection of lipids in positive ionisation mode. To overcome the hardness of oat grains and fragility of oat tissue sections, sectioning and sample preparation methods were also optimised, with gelatin-coating of ITO glass slides prior to mounting found to minimise sample tearing. To improve the detection of TGs, the concentration of sodium was adjusted in the preparation of MALDI matrix, with 100 mM NaCl performing best for lipid identification and signal intensity. The detection of lipids was enhanced with activation of the TIMS feature, where signals improved further, and more lipid species could be identified. As previously reported, the majority of lipids localise, but are not restricted to the endosperm region of oat grains. Our study demonstrates for the first time, the capability of MALDI-TIMS-MSI in providing more accurate analysis of lipids by distinguishing and localising isobaric and isomeric lipids in oats. This study may be used to inform future, advanced evaluation of lipids, particularly TGs and PCs, in oats sampled across development stages and from different varieties. This novel lipid analysis workflow, including sample preparation of oat sections, may also pave the way for more in-depth research into discovering lipid biomarkers for grain quality, developing novel oat processing techniques for metabolite enrichment, or implementing breeding strategies to cultivate nutritionally superior varieties.

CRediT authorship contribution statement

Wai C.D. Lau: Conceptualization, Methodology, Investigation, Formal analysis, Validation, Visualization, Writing – original draft. **Leigh Donnellan:** Conceptualization, Methodology, Formal analysis, Writing – review & editing. **Matthew Briggs:** Conceptualization, Methodology, Formal analysis, Writing – review & editing. **Thusitha Rupasinghe:** Methodology, Formal analysis. **John C. Harris:** Writing – review & editing, Supervision. **Julie E. Hayes:** Writing – review & editing, Supervision. **Peter Hoffmann:** Conceptualization, Writing – original draft, Supervision, Funding acquisition, Project administration.

Declaration of Competing Interest

The authors declare that they have no known competing financial interests or personal relationships that could have appeared to influence the work reported in this paper.

Data availability

Data will be made available on request.

Acknowledgement

The authors acknowledge Bioplatforms Australia, the University of South Australia, and the State and Federal Governments for the co-funding of the NCRIS-enabled Mass Spectrometry and Proteomics facility at the University of South Australia. ARC LIEF LE200100183 provided the funding for the timsTOF *flex* mass spectrometer (Bruker Daltonics). The authors wish to thank the Federal Government and University of South Australia for awarding the Research Training Program (International) Scholarship. This work was also supported and supervised by Prof. Maria Saarela and Dr John Carragher from the South Australian Research and Development Institute (SARDI).

Appendix A. Supplementary data

Supplementary data to this article can be found online at https://doi.org/10.1016/j.foodchem.2023.137275.

References

Amiri, R., Farrokhpour, H., & Tabrizchi, M. (2021). Sodium salts effect on the time of flight mass spectra of some amino acids in the direct-laser desorption ionization and matrix-assisted laser desorption/ionization. *Journal of the Chinese Chemical Society (Taipei), 68*(7), 1263–1270. https://doi.org/10.1002/jccs.202000400

Banaś, A., Debski, H., Banaś, W., Heneen, W. K., Dahlqvist, A., Bafor, M., … Stymne, S. (2007). Lipids in grain tissues of oat (Avena sativa): Differences in content, time of deposition, and fatty acid composition. *Journal of Experimental Botany, 58*(10), 2463–2470. https://doi.org/10.1093/jxb/erm125

Boskamp, M. S., & Soltwisch, J. (2020). Charge Distribution between Different Classes of Glycerophospolipids in MALDI-MS Imaging. *Analytical Chemistry, 92*(7), 5222–5230. https://doi.org/10.1021/acs.analchem.9b05761

Boughton, B. A., Thinagaran, D., Sarabia, D., Bacic, A., & Roessner, U. (2015). Mass spectrometry imaging for plant biology: A review. *Phytochemistry Reviews, 15*(3), 445–488. https://doi.org/10.1007/s11101-015-9440-2

Dąbrowski, G., & Konopka, I. (2022). Update on food sources and biological activity of odd-chain, branched and cyclic fatty acids — A review. *Trends in Food Science & Technology, 119*, 514–529. https://doi.org/10.1016/j.tifs.2021.12.019

Dong, Y., Li, B., Malitsky, S., Rogachev, I., Aharoni, A., Kaftan, F., … Franceschi, P. (2016). Sample preparation for mass spectrometry imaging of plant tissues: A review. *Frontiers in Plant Science, 7*(2016), 60. https://doi.org/10.3389/fpls.2016.00060

Dufresne, M., Patterson, N. H., Norris, J. L., & Caprioli, R. M. (2019). Combining Salt Doping and Matrix Sublimation for High Spatial Resolution MALDI Imaging Mass Spectrometry of Neutral Lipids. *Analytical Chemistry, 91*(20), 12928–12934. https://doi.org/10.1021/acs.analchem.9b02974

Feenstra, A. D., Alexander, L. E., Song, Z., Korte, A. R., Yandeau-Nelson, M. D., Nikolau, B. J., & Lee, Y. J. (2017). Spatial Mapping and Profiling of Metabolite Distributions during Germination. *Plant Physiology, 174*(4), 2532–2548. https://doi.org/10.1104/pp.17.00652

Fenyk, S., Woodfield, H. K., Romsdahl, T. B., Wallington, E. J., Bates, R. E., Fell, D. A., … Harwood, J. L. (2022). Overexpression of phospholipid: Diacylglycerol acyltransferase in Brassica napus results in changes in lipid metabolism and oil accumulation. *Biochemical Journal, 479*(6), 805–823. https://doi.org/10.1042/BCJ20220003

Fu, T., Oetjen, J., Chapelle, M., Verdu, A., Szesny, M., Chaumot, A., … Ayciriex, S. (2020). In situ isobaric lipid mapping by MALDI–ion mobility separation–mass spectrometry imaging. *Journal of Mass Spectrometry, 55*(9), e4531-n/a. https://doi.org/10.1002/jms.4531

Gangopadhyay, N., Hossain, M. B., Rai, D. K., & Brunton, N. P. (2015). A review of extraction and analysis of bioactives in oat and barley and scope for use of novel food processing technologies. *Molecules, 20*(6), 10884–10909. https://doi.org/10.3390/molecules200610884

Gidden, J., Liyanage, R., Durham, B., & Lay, J. O., Jr (2007). Reducing fragmentation observed in the matrix-assisted laser desorption/ionization time-of-flight mass spectrometric analysis of triacylglycerols in vegetable oils. *Rapid Communications in Mass Spectrometry, 21*(13), 1951–1957. https://doi.org/10.1002/rcm.3041

Gorzolka, K., Kölling, J., Nattkemper, T. W., & Niehaus, K. (2016). Spatio-Temporal metabolite profiling of the barley germination process by MALDI MS imaging. *PLoS One1, 11*(3), e0150208–e. https://doi.org/10.1371/journal.pone.0150208

Helmer, P. O., Nordhorn, I. D., Korf, A., Behrens, A., Buchholz, R., Zubeil, F., … Hayen, H. (2021). Complementing Matrix-Assisted Laser Desorption Ionization-Mass Spectrometry Imaging with Chromatography Data for Improved Assignment of Isobaric and Isomeric Phospholipids Utilizing Trapped Ion Mobility-Mass Spectrometry. *Analytical Chemistry, 93*(4), 2135–2143. https://doi.org/10.1021/acs.analchem.0c03942

Heneen, W. K., Banas, A., Leonova, S., Carlsson, A. S., Marttila, S., Debski, H., & Stymne, S. (2009). The distribution of oil in the oat grain. *Plant Signaling & Behavior, 4*(1), 55–56. https://doi.org/10.1007/s00425-008-0

Kim, I., Kim, S., Shin, D., & Kim, J. (2016). Matrix Additives in MALDI-TOF MS Analysis of Glycans. *Bulletin of the Korean Chemical Society, 37*(1), 105–107. https://doi.org/10.1002/bkcs.10617

Kokesch-Himmelreich, J., Wittek, O., Race, A. M., Rakete, S., Schlicht, C., Busch, U., & Römpp, A. (2022). MALDI mass spectrometry imaging: From constituents in fresh food to ingredients, contaminants and additives in processed food. *Food Chemistry, 385*, 132529. https://doi.org/10.1016/j.foodchem.2022.132529

Laskowski, W., Górska-Warsewicz, H., Rejman, K., Czeczotko, M., & Zwolińska, J. (2019). How important are cereals and cereal products in the average polish diet? *Nutrients, 11*(3), 679. https://doi.org/10.3390/nu11030679

Lee, Y.-R., Briggs, M. T., Kuliwaba, J. S., Anderson, P. H., Condina, M. R., & Hoffmann, P. (2021). Gelatin-coated indium tin oxide slides improve human cartilage-bone tissue adherence and N-glycan signal intensity for mass spectrometry imaging. *Analytical and Bioanalytical Chemistry, 413*(10), 2675–2682. https://doi.org/10.1007/s00216-020-02986-x

Leopold, J., Popkova, Y., Engel, K. M., & Schiller, J. (2018). Recent developments of useful MALDI matrices for the mass spectrometric characterization of lipids. *Biomolecules, 8*(4), 173. https://doi.org/10.3390/biom8040173

Liu, B., Wang, X., Li, K., & Cai, Z. (2021). Spatially Resolved Metabolomics and Lipidomics Reveal Salinity and Drought-Tolerant Mechanisms of Cottonseeds. *Journal of Agricultural and Food Chemistry, 69*(28), 8028–8037. https://doi.org/10.1021/acs.jafc.1c01598

May, J. C., Goodwin, C. R., Lareau, N. M., Leaptrot, K. L., Morris, C. B., Kurulugama, R. T., … McLean, J. A. (2014). Conformational Ordering of Biomolecules in the Gas Phase: Nitrogen Collision Cross Sections Measured on a Prototype High Resolution Drift Tube Ion Mobility-Mass Spectrometer. *Analytical Chemistry, 86*(4), 2107–2116. https://doi.org/10.1021/ac4038448

Michelmann, K., Silveira, J. A., Ridgeway, M. E., & Park, M. A. (2015). Fundamentals of Trapped Ion Mobility Spectrometry. *Journal of the American Society for Mass Spectrometry, 26*(1), 14–24. https://doi.org/10.1007/s13361-014-0999-4

Montini, L., Crocoll, C., Gleadow, R. M., Motawia, M. S., Janfelt, C., & Bjarnholt, N. (2020). Matrix-Assisted Laser Desorption/Ionization-Mass Spectrometry Imaging of Metabolites during Sorghum Germination. *Plant Physiology, 183*(3), 925–942. https://doi.org/10.1104/pp.19.01357

Paglia, G., Angel, P., Williams, J. P., Richardson, K., Olivos, H. J., Thompson, J. W., … Astarita, G. (2015). Ion Mobility-Derived Collision Cross Section As an Additional Measure for Lipid Fingerprinting and Identification. *Analytical Chemistry, 87*(2), 1137–1144. https://doi.org/10.1021/ac503715v

Paglia, G., Williams, J. P., Menikarachchi, L., Thompson, J. W., Tyldesley-Worster, R., Halldórsson, S. D., … Astarita, G. (2014). Ion Mobility Derived Collision Cross Sections to Support Metabolomics Applications. *Analytical Chemistry, 86*(8), 3985–3993. https://doi.org/10.1021/ac500405x

Rasane, P., Jha, A., Sabikhi, L., Kumar, A., & Unnikrishnan, V. S. (2015). Nutritional advantages of oats and opportunities for its processing as value added foods - a review. *Journal of Food Science and Technology, 52*(2), 662–675. https://doi.org/10.1007/s13197-013-1072-1

Ridgeway, M. E., Lubeck, M., Jordens, J., Mann, M., & Park, M. A. (2018). Trapped ion mobility spectrometry: A short review. *International Journal of Mass Spectrometry, 425*, 22–35. https://doi.org/10.1016/j.ijms.2018.01.006

Righetti, L., Bhandari, D. R., Rolli, E., Tortorella, S., Bruni, R., Dall'Asta, C., & Spengler, B. (2021). Mycotoxin Uptake in Wheat — Eavesdropping Fusarium Presence for Priming Plant Defenses or a Trojan Horse to Weaken Them? *Frontiers in plant science, 12*, 711389. https://doi.org/10.3389/fpls.2021.711389

Righetti, L., Gottwald, S., Tortorella, S., Spengler, B., & Bhandari, D. R. (2022). Mass Spectrometry Imaging Disclosed Spatial Distribution of Defense-Related Metabolites in Triticum spp. *Metabolites, 12*(1), 48. https://doi.org/10.3390/metabo12010048

Spraggins, J. M., Djambazova, K. V., Rivera, E. S., Migas, L. G., Neumann, E. K., Fuetterer, A., … Caprioli, R. M. (2019). High-Performance Molecular Imaging with MALDI Trapped Ion-Mobility Time-of-Flight (timsTOF) Mass Spectrometry. *Analytical Chemistry, 91*(22), 14552–14560. https://doi.org/10.1021/acs.analchem.9b03612

Sturtevant, D., Lee, Y.-J., & Chapman, K. D. (2015). Matrix assisted laser desorption/ionization-mass spectrometry imaging (MALDI-MSI) for direct visualization of plant metabolites in situ. *Current Opinion in Biotechnology, 37*(C), 53–60. https://doi.org/10.1016/j.copbio.2015.10.004

Tsugawa, H., Cajka, T., Kind, T., Ma, Y., Higgins, B., Ikeda, K., … Arita, M. (2015). MS-DIAL: Data-independent MS/MS deconvolution for comprehensive metabolome analysis. *Nature Methods, 12*(6), 523–526. https://doi.org/10.1038/nmeth.3393

Vasilopoulou, C. G., Sulek, K., Brunner, A.-D., Meitei, N. S., Schweiger-Hufnagel, U., Meyer, S. W., … Meier, F. (2020). Trapped ion mobility spectrometry and PASEF enable in-depth lipidomics from minimal sample amounts. *Nature Communications, 11*(1), 331. https://doi.org/10.1038/s41467-019-14044-x

Woodfield, H. K., Sturtevant, D., Borisjuk, L., Munz, E., Guschina, I. A., Chapman, K., & Harwood, J. L. (2017). Spatial and Temporal Mapping of Key Lipid Species in Brassica napus Seeds. *Plant Physiology, 173*(4), 1998–2009. https://doi.org/10.1104/pp.16.01705

Yoshimura, Y., & Zaima, N. (2020). Application of mass spectrometry imaging for visualizing food components. *Foods, 9*(5), 575. https://doi.org/10.3390/foods9050575

Yoshimura, Y., Zaima, N., Moriyama, T., & Kawamura, Y. (2012). Different localization patterns of anthocyanin species in the pericarp of black rice revealed by imaging mass spectrometry. *PLoS One1, 7*(2), e31285–e. https://doi.org/10.1371/journal.pone.0031285

Zhang, Y.-X., Zhang, Y.-D., & Shi, Y.-P. (2023). A reliable and effective sample preparation protocol of MALDI-TOF-MSI for lipids imaging analysis in hard and dry cereals. *Food Chemistry, 398*, 133911. https://doi.org/10.1016/j.foodchem.2022.133911

Zhou, M., Robards, K., Glennie-Holmes, M., & Helliwell, S. (1999). Oat lipids. *Journal of the American Oil Chemists' Society, 76*(2), 159–169. https://doi.org/10.1007/s11746-999-0213-1